Development of neutron reflectometry for a HiCANS: the HERMES instrument at the JULIC Neutron Platform

Mariano Andrés Paulin[1*], *Ivan* Pechenizkiy[2], *Paul* Zakalek[2], *Klaus* Lieutenant[2], *Peter* Kämmerling[2], *Alexander* Steffens[2], *Harald* Kleines[2], *Ulrich* Rücker[2], *Thomas* Gutberlet[2], *Sébastien* Gautrot[1], *Alain* Menelle[1], and *Frédéric* Ott[1, 3]

[1] Laboratoire Léon Brillouin, UMR12 CEA-CNRS, 91191 Gif sur Yvette Cedex, France
[2] Jülich Centre for Neutron Science, FZJ, 52428 Jülich, Germany
[3] Université Paris Saclay, 91191 Gif sur Yvette Cedex, France

Abstract. High Current Compact Accelerator-driven Neutron Sources (HiCANS) have recently emerged as a possible solution to the drop in neutron provision in Europe due to the closure of several research reactors. Within this new trend, the Laboratoire Léon Brillouin (LLB) is currently assessing the performance of neutron techniques around this novel type of source. HERMES is a time-of-flight horizontal reflectometer that was operated by the LLB at the ORPHEE reactor until 2019 and was dedicated to soft matter studies. Through a collaboration with the Jülich Centre for Neutron Science, HERMES was installed in 2022 at the JULIC Neutron Platform (JNP) at the Forschungszentrum Jülich. This platform is able to deliver neutron pulses in the *100 μs - 2 s* range and is very well suited to evaluate the feasibility of reflectivity experiments at a HiCANS. Since its installation and first tests in 2022, several improvements have been implemented at HERMES. Our current goal is to perform reflectivity experiments with large neutron mirrors as a proof of concept, as the flux at the JNP is several orders of magnitude lower than the original ORPHEE flux or the one expected at a HiCANS. Nevertheless, Monte Carlo simulations show that an instrument as HERMES operating at a HiCANS could match the performance of similar instruments at research reactors and spallation sources.

1 Introduction

The neutron scattering ecosystem is in the present dominated by reactor-based and spallation sources. In both cases, construction and operation costs are high and decommissioning is a major challenge mainly due to the high activation. In that context, HiCANS are quite appealing due to reduced costs at comparable performances. Earlier experience in compact accelerator-driven neutron sources [1, 2, 3] created the foundations for the current developments. Within Europe, several projects aiming at building national neutron scattering sources are at different stages of development [4-10]. These efforts are clustered within the European Low Energy accelerator-driven Neutron facilities Association (ELENA) [11].

In France, the potential of HiCANS is being evaluated with the goal of providing the national neutron scattering community with a suite of competitive instruments. Typically, Monte Carlo simulations [12, 13] are used to estimate the performances of neutron sources and scattering instruments. However, as HiCANS are a new type of source, experimental validation of the simulated performances is necessary.

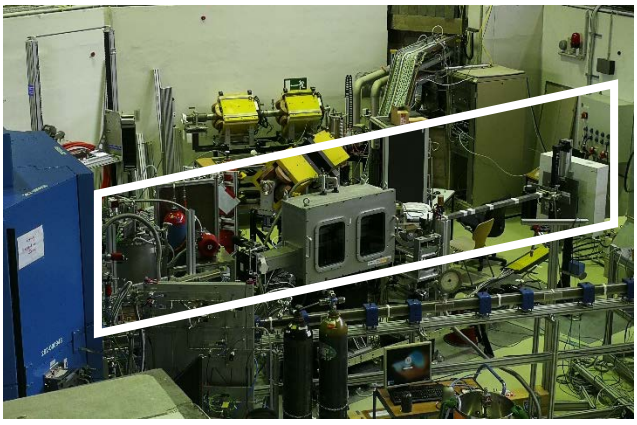

Fig. 1. The HERMES reflectometer at the JULIC Neutron Platform.

* Corresponding author: mariano.paulin@cab.cnea.gob.ar

As a tool to validate the simulations and test different aspects of the technique at a HiCANS, the HERMES reflectometer was installed [14] at the JULIC Neutron Platform (JNP) at the JULIC (JÜlich Light Ion Cyclotron) accelerator [15] of the Institute for Nuclear Physics (IKP) of Forschungszentrum Jülich.

HERMES [16-18] was conceived as a time-of-flight horizontal sample reflectometer (see Fig.1) mainly intended for soft matter studies and it was in operation at the Orphée reactor [19] until its shutdown in 2019.

The JNP shown in Figure 1 was developed as a technological test platform for the High Brilliance Neutron Source project (HBS) [8, 9, 20].

The IKP built a dedicated proton beamline to extract 45 MeV protons from the JULIC accelerator and inject them onto the target-moderator-reflector (TMR) assembly built by JCNS. Neutrons are generated by the impact of protons on a water-cooled tantalum target and moderated by a polyethylene (PE) block surrounded by a lead reflector. The TMR assembly is embedded in a multilayer shielding (Pb/borated PE) with eight extraction channels designed to fit several instruments. Furthermore, the TMR assembly can accommodate individual cold moderators in each channel.

The JNP source delivers cold neutrons with pulses in the 100 μs – 2 s range and thus, is very well suited to perform time-of-flight (ToF) reflectivity experiments. As it was stated in a previous article [14], reflectivity measurements are particularly useful for evaluating the performances of a HiCANS source including the assessment of background noise.

2 Experimental setup

2.1 Neutron source and guide system

Initial HERMES experiments at the JNP [14] were performed with the reflectometer fed by the PE thermal moderator. In July of 2023, a para-H_2 cold moderator [21, 22, 23] was installed at the extraction channel 3 of the TMR, providing HERMES with a cold spectrum more suited for reflectometry studies. A 2.5 m neutron guide with m = 1.2 on all sides transports the neutrons out of the target shielding and into HERMES.

2.2 Instrument

A 20 cm gap was left between the end of the neutron guide and the collimator to be able to fit a frame-overlap chopper in the future. Collimation is achieved with a set of four variable slits with a maximum collimation distance (d_{14}) of 1.5 m. The slits have a 30 mm horizontal opening and a motorized variable vertical opening (0.5-10mm).

Two horizontal m = 3.5 supermirrors situated between slits 2, 3 and 4 can be used to deflect the beam for air-liquid reflectivity experiments. Vertical $m = 2$ supermirrors transport the beam along the collimator to exploit the beam's horizontal divergence. A schematic view of the instrument is shown in Figure 2 including its principal dimensions.

The sample sits at a distance of 40 cm from the last slit. An “anti-background” slit with an adjustable vertical opening is positioned at 15 cm from the center of the sample. Finally, a single ^{3}He tube detector (P = 10 bar) shielded with B_4C is located at 2 m from the sample position.

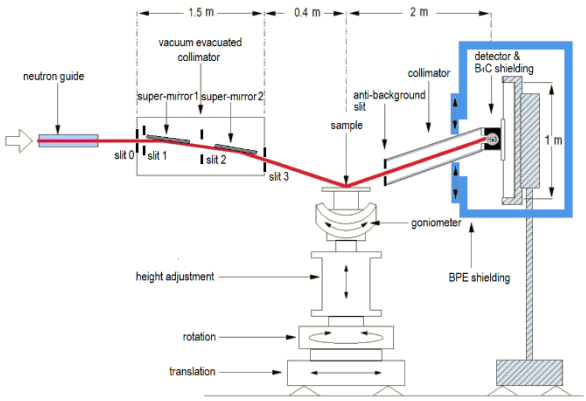

Fig. 2. Scheme of the HERMES reflectometer.

The beam reflected by the sample has a rather high horizontal divergence (1-3°) and thus a large detector would be needed to count all the reflected neutrons. A neutron guide with m = 2 supermirrors on the sides and shielded with B_4C is placed between the “anti-background” slit and the detector. This guide acts as a collimator for the reflected beam, harnessing all its horizontal divergence with a rather small detector area thus avoiding the background signal due to spurious neutrons arriving at the detector. The total flight path of the instrument is 7 m.

3 Experiments at the JULIC neutron platform

First experiments with HERMES at the JNP in 2022 [14] were carried out not only without a cold moderator but also with a low proton current ($I_p \approx 200$ nA) impinging into the target. Due to the improvements made in the JULIC accelerator at the beginning of 2023, it was possible to increase the proton current up to $I_p = 3.5$ µA. On top of that, the installation of a cylindrical (d = 2 cm, l = 10 cm) para-H_2 cold moderator operating at 25 K in July 2023 further improved the total flux and usefulness of the spectrum.

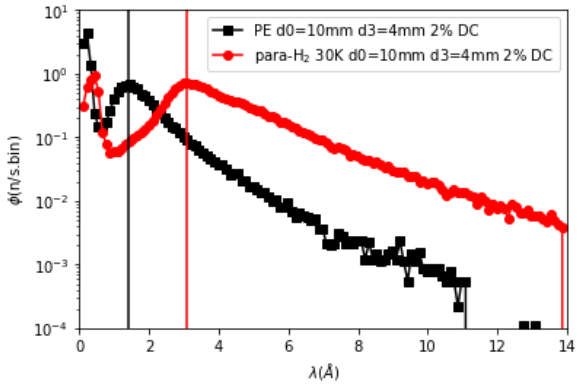

Fig. 3. Direct beam measured at the HERMES reflectometer in 2023 with and without a cold moderator, normalized for a proton current of $I_p = 3.5$ µA.

As it is shown in Figure 3, the para-H_2 moderator shifts the neutron flux peak λ_{peak} from 1.4 Å to 3.1 Å and increases the total amount of neutrons in the 1-12 Å range from 0.74(1) n/s.cm^2.µA to 1.69(1) n/s.cm^2.µA, which represents a 2.3 gain factor. The gain is partially due to a better transport of neutrons done by the guide and to the inner characteristics of the para-H_2 cylindrical moderator [21, 22, 23].

3.1 m=4 supermirror

The S-DH m=4 supermirror that was originally measured in December of 2022 [14] was remeasured as a means to compare the performance evolution of the instrument since its installation at JNP.

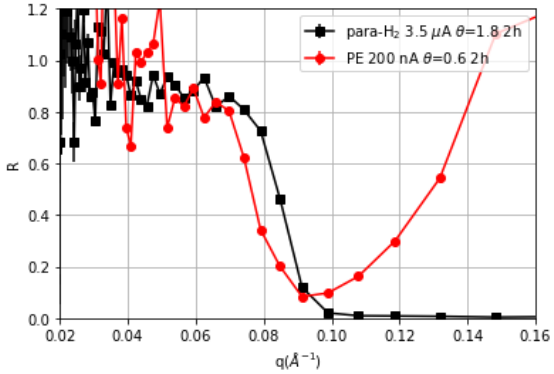

Fig. 4. A S-DH m=4 supermirror reflectivity measured at the HERMES reflectometer without the cold moderator (200 nA, 125 Hz, 400 µs , θ_{in}=0.6°) and with the cold moderator (3.5 µA, 25 Hz, 800 µs, θ_{in}=1.8°). Para-H_2 measurement was re-binned to match the PE experiment.

The improvements in the instrument's performance since its installation are clearly seen in Figure 4. The statistics were increased thanks to the higher proton current and the installation of the cold moderator. The use of cold neutrons allowed us to use a higher incident angle θ_{in}=1.8° which results in an improvement in angular resolution, allowing us to get a better-defined critical edge. At the same time, as the neutron peak flux for the para-H_2 moderator is further away from the prompt pulse than in the case of PE (see Fig. 3), we are able to measure the critical edge of the m=4 SM without the artificial rise in reflectivity seen in the PE measurement for q > 0.1 Å^{-1}.

3.2 40nm Ni layer on Si

Taking advantage of the improved performance of the instrument, we measured a 40 nm Ni layer on Si (12 cm x 3 cm), its reflectivity is shown in Figure 5.

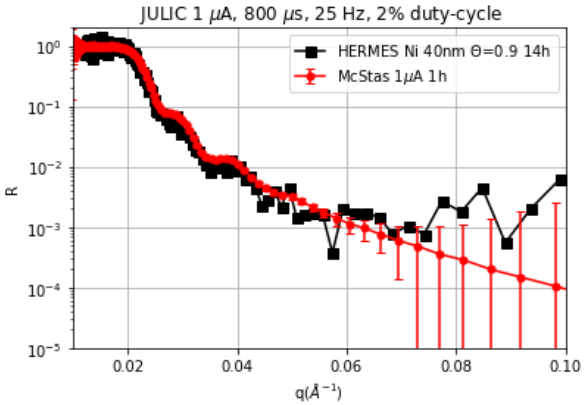

Fig. 5. Reflectivity of a 40 nm Ni layer on Si measured at HERMES reflectometer at the JNP without additional detector shielding and the corresponding McStas simulation. Error bars for the McStas simulation are estimated for a 1 h measurement.

During this experiment, the proton current was only 1 μA, and thus, 14 h were required to collect enough statistics. We were able to measure reflectivities down to 10^{-3} with approximately 1 W of power onto the target. The simulated curve (McStas) fits our experiment, although above q = 0.04 $Å^{-1}$ the effects of background become noticeable for the experimental curve.

3.3 Frame-overlap mirror

Currently, due to radioprotection limitations, the maximum duty cycle of the JNP is limited to 2%. Nevertheless, higher duty cycles could be used to increase the total flux in the sample, improving the statistics. If we want to keep the wavelength resolution constant, increasing the pulse length is not an option but it could be possible to increase the repetition rate. In this case, frame-overlap becomes an issue and measures should be taken to minimize it.

The most common way is to install a frame-overlap chopper somewhere along the neutron path synchronized with the source to eliminate the slowest neutrons and thus the FO effect. Another approach is to install a mirror at a fixed angle that reflects the longest wavelength neutrons. For that purpose, we built a special holder to accommodate and align 5 individual 0.5mm Si wafers (4 cm x 9 cm) and create a 45 cm Si mirror. We installed it at the HERMES collimator in the position of the 2nd deflecting supermirror (see Fig. 2) at an incidence angle of 0.3°.

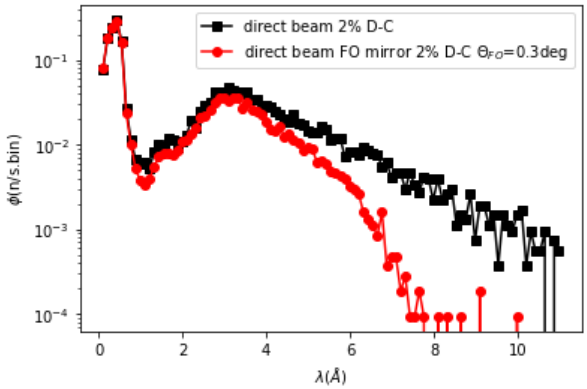

Fig. 6. Direct beam with and without a 0.5 mm Si frame-overlap mirror installed at a 0.3º angle with respect to the neutron beam.

In Figure 6 the direct beam with and without the mirror is shown. Due to the relaxed collimation (α_{max}=0.08°), chosen to keep statistics as high as possible, the cut-off above 6 Å is not totally sharp. Nevertheless, a reduction by almost 2 orders of magnitude in neutron counts is obtained with this simple device. Setting the frame overlap limit at 8 Å with such a mirror would allow us to work at frequencies up to 70 Hz (flight time (8Å) = 7[m]/485[m/s] = 14 ms; f = 70 Hz) which is a factor 3 higher than the current setting.

3.4 Shielding

The instrument's performance strongly relies on the background-to-signal ratio and therefore, efforts must be focused on properly shielding the instrument from external background sources. The HERMES shielding was conceived for its installation at the guide hall of ORPHEE where background levels were very low with virtually no fast and epithermal neutron background. The original shielding consisted of a 10mm thick boroflex (50 wt% B_4C, 50 wt% rubber) box surrounding the He3 detector with a 10 mm x 30 mm opening in the front where the collimator coming from the sample was inserted (see Fig. 1). At JNP on the contrary, HERMES is located in the same bunker as the proton beamline and the

target station. During neutron production, there is a very high fast neutron background (prompt pulse). This background decays quickly, but the moderation of fast neutrons in the bunker concrete creates a cloud of thermal neutrons, which decays only over millisecond timescales. In order to shield the detector from these unwanted neutrons, we designed and built an additional 20 mm thick borated polyethylene (BPE) shielding box (see Fig. 7) that encloses the whole detector setup, including the detector, its original shielding, and allows the detector's vertical movement.

Fig. 7. New BPE (blue) shielding box added to the HERMES detector.

The background-to-signal ratio excluding the prompt pulse (ToF > 2.5 ms, λ > 1.4 Å) was reduced by 2 orders of magnitude from 3.10^{-3} to 4.10^{-5} just by the addition of the 20 mm BPE (16.1 wt% B_2O_3 and 83.9 wt% PE). Although these values are still higher than the original values at ORPHEE, there is still a margin of progress in the accelerator and TMR shielding. The shielding proposed for ICONE and HBS would include an additional heavy concrete casemate separating the TMR station from the instruments.

4 Monte Carlo simulations

4.1 Reflectivity for a 40 nm Ni layer

Monte Carlo ray tracing simulations were carried out to evaluate the instrument performance using McStas [12]. Three different source scenarios were considered for this simulation, in all three scenarios the current HERMES configuration was used. The first one is the best-case scenario expected for the JULIC Neutron Platform, which has not been achieved yet due to technical and radioprotection limitations. The second scenario is the one for ICONE [4], the projected French national neutron source. The last one is the projected flux for the High Brilliance Neutron Source (HBS) [24].

The source is modelled with three components (Maxwellian) corresponding to the cold-moderated neutrons (60 K), the thermal-moderated neutrons (305 K), and the under-moderated ones (UM). In the three cases, the flux is calculated considering a para-H_2 cold moderator at 20 K inserted in the extraction plug dedicated to the instrument.
For these simulations, we chose a 10 cm x 10 cm sample (beam is only 3 cm wide) consisting of a 40 nm Ni layer on Si. Due to ToF resolution limitations with long pulses (800 µs), in the case of ICONE and HBS, a shorter pulse length (208 and 200 µs) pulse length was chosen to gain resolution.

In Table 1, the estimated flux at the source and the sample position is presented for the three scenarios.

Table 1. Estimated flux at the source and the sample position for the JNP, ICONE, and HBS at their maximum duty cycle (DC).

Source	E [MeV]	Ip [mA]	DC [%]	ϕ_{source} [n/s.cm^2]	ϕ_{sample} [n/s.cm^2]
JNP	45	0.006	5	7.52 10^4(1)	1.07 10^3(1)
ICONE	30	100	4	7.44 10^8(1)	1.07 10^7(1)
HBS	70	90	1.6	1.19 10^9(1)	1.70 10^7(1)

In Figure 8, we show the simulated reflectivity curve for the JNP, ICONE, and HBS configuration for a θ = 0.8° incident angle.

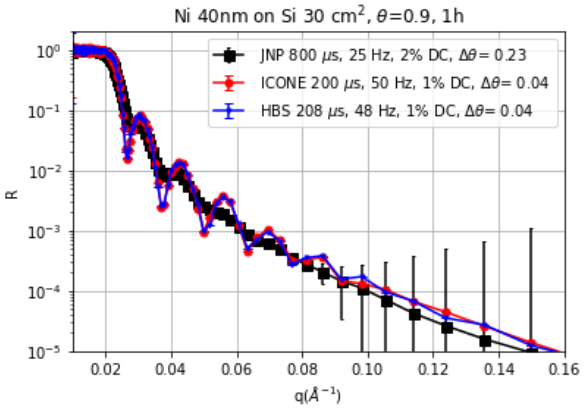

Fig. 8. Simulated reflectivity curve for a 40 nm Ni layer on Si on HERMES at JNP, ICONE and HBS.

Error bars were estimated assuming a 1 h collecting time. The Kiessig fringes are noticeable below q = 0.1 Å^{-1}, and reflectivities down to 10^{-4} should be measurable at JNP provided that the background noise is kept low enough. In the case of ICONE and HBS, statistics does not represent an issue to easily achieve reflectivities below 10^{-5}.

5 Conclusions

The JNP represents an opportunity to test the operation of neutron scattering instrumentation to be installed at HiCANS. Its flexibility allowed us to test many features that are critical for the future developments.

Since the first neutrons were produced in 2022, several improvements were implemented to the platform, including additional shielding and the incorporation of a dedicated para-H_2 cold source for HERMES.

The instruments performance was vastly improved by these upgrades. The increase in proton current (I_p) followed by the spectrum shift towards colder neutrons allowed us to increase the reflectivity range of the instrument. This was also made possible by a reduction in background noise levels thanks to the added accelerator heavy concrete shielding and additional 20mm borated polyethylene added to the HERMES detector.

If we focus on the 40 nm Ni layer (Fig. 5), almost 3 orders in reflectivity were achieved in a 14h experiment with only 1 W into the target. Scaling these data to the 100 kW that is foreseen for a HiCANS, we should be able to achieve 6 orders in reflectivity for a 1 cm^2 sample in a 1 h measurement.

If we extrapolate the last HERMES results at the JNP with the Monte Carlo simulations for ICONE and HBS, we can envision that instruments performance at a HiCANS would compare well with those that are currently operating at research reactors or spallation sources.

Acknowledgments This work is part of the collaboration within ELENA and LENS on the development of HiCANS. It has been funded by the “CANS Inflexion” program at the CEA and the “IPHI-Neutron” SESAME project of the Île de France region.

References

1. D. V. Baxter, Neutron News **31**, 2-4, 44-47 (2020)
2. Y. Otake, Neutron News **31**, 2-4, 32-36 (2020)
3. M. Furusakaa, H. Satoa, T. Kamiyamaa, M. Ohnumaa, Y Kiyanagi, Phys. Procedia 60, 167-174 (2014)
4. F. Ott, M. Plazanet, ICONE, une nouvelle source de diffusion neutronique française, https://2fdn.cnrs.fr/wp-content/uploads/2023/09/ICONE-digital.pdf (2023)
5. F. Ott, J. Darpentigny, B. Annighöfer, M. A. Paulin, J-L. Meuriot, A. Menelle, N.Sellami, J. Schwindling, EPJ Web of Conferences **286**, 02001 (2023)
6. T. Gutberlet, U. Rücker, P. Zakalek, T. Cronert, J. Voigt, J. Baggemann, P.E. Doege, E. Mauerhofer, S. Böhm, J.P. Dabruck, R. Nabbi, M. Butzek, M. Klaus, C. Lange, T. Brückel, Phys. B: Condens. Matter **570**, 345-348 (2019)
7. T. Gutberlet, U. Rücker, E. Mauerhofer, P.Zakalek, T. Cronert, J. Voigt , J. Baggemann, J. Li, P. Doege, S. Böhm, M. Rimmler, O. Felden, R. Gebel, O. Meusel, H. Podlech , W. Barth, T. Brückel, Neutron News **31**, 37-43 (2020)
8. T. Brückel, T. Gutberlet, J. Baggemann, J. Chen, T. Claudio-Weber, Q. Ding, M. El-Barbari, J. Li, K. Lieutenant, E. Mauerhofer, U. Rücker, N. Schmidt, A. Schwab, J. Voigt, P. Zakalek, Y. Bessler, R. Hanslik, R. Achten, F. Löchte, M. Strothmann, O. Felden, R. Gebel, A. Lehrach, M. Rimmler, H. Podlech, O. Meusel, F. Ott, A. Menelle, M. A. Paulin, EPJ Web of Conferences **286**, 02001 (2023)

9. P. Zakalek, R. Achten, J. Baggemann, Y. Beßler, F. Beule, T. Brückel, J. Chen, Q. Ding, M. El-Barbari, R. Engels, O. Felden, R. Gebel, K. Grigoryev, T. Gutberlet, R. Hanslik, V. Kamerdzhiev, P. Kämmerling, H. Kleines, J. Li, K. Lieutenant, F. Löchte, E. Mauerhofer, M. A. Paulin, I. Pechenizkiy, U. Rücker, N. Schmidt, A. Schwab, A. Steffens, F. Ott, Y. Valdau, E. Vezhlev, J. Voigt, EPJ Web of Conferences **286**, 02004 (2023)
10. M. Pérez, F. Sordo, I. Bustinduy, J.L. Muñoz, F. J. Villacorta, Neutron News **31**, 2-4, 19-25 (2020)
11. http://www.elena-neutron.eu
12. P. Willendrup, K. Lefmann, J. of Neutron Res. **22**, 1-16 (2020)
13. J. F. Briesmeister, T. E. Booth, D. G. Collins, J. J. Devaney, G. P. Estes, H. M. Fisher, R. A. Forster III, T. N. K. Godfrey, J. S. Hendricks, H. G. Hughes III, R. C. Little, R. E. Prael, R. G. Schrandt, R. E. Seamon, E. C. Snow, W. L. Thompson, W. T. Urban, J. T. West, MCNP—A General Monte Carlo Code for Neutron and Photon Transport, Los Alamos National Laboratory Tech. Rep. LA-7396-M, Rev. 2 (1986)
14. M. A. Paulin, I. Pechenizkiy, P. Zakalek, K. Lieutenant, P. Kämmerling, A. Steffens, H. Kleines, U. Rücker, T. Gutberlet, S. Gautrot, A. Menelle, F. Ott, , EPJ Web of Conferences **286**, 03003 (2023)
15. O. Felden, N. Demary, N.-O. Fröhlich, R. Gebel, M. Rimmler, Y. Valdau, 22nd Int. Conf. on Cyclotrons and their Applications, doi:10.18429/JACoW-Cyclotrons2019-TUP019 (2019),
16. F. Cousin, F. Ott, F. Gibert, A. Menelle, Eur. Phys. J. Plus **126**, 109 (2011)
17. G. Battaglin, A. Menelle, M. Montecchi, E. Nichelatti, P. Polato, Glass Technol. **43**, 203-208 (2002)
18. D. Lairez, A. Chennevière, F. Ott, J. Appl. Crystallogr. **53**, 464-476 (2020)
19. B. Farnoux, D. Cribier, Phys. B+C **120**, 31-36 (1983)
20. T. Brückel, T. Gutberlet, Conceptual Design Report Jülich High Brilliance Neutron Source (HBS) **8,** ISBN: 978-3-95806-501-7 (2020)
21. T. Kai, M. Harada, M. Teshigawara, N. Watanabe, Y. Ikeda, Nucl. Instrum. Methods Phys. Res. **523**, 398-414 (2004)
22. T. Brückel, T. Gutberlet, R. Achten, Y. Bessler, R. Hanslik, H. Kleines, J. Li, K. Lieutenant, F. Löchte, I. Pechenizkiy, E. Vezhlev, J. Voigt, J. Wolters, J. Baggemann, E. Mauerhofer, U. Rücker, P. Zakalek, Technical Design Report HBS **2,** doi:10.34734/FZJ-2023-03723 (2023)
23. S. Eisenhut, M. Klaus, J. Baggemann, U. Rücker, Y. Beßler, A. Schwab, C. Haberstroh, T. Cronert, T. Gutberlet, T. Brückel, C. Lange, EPJ Web of Conferences **231**, 04001 (2020)
24. T. Brückel, T. Gutberlet, K. Lieutenant, J. Voigt, et al, Technical Design Report HBS **3**, doi:10.34734/FZJ-2023-03724 (2023)